Supplementary Material for "Functional Recovery in New Mouse Models of ALS/FTLD after Clearance of Pathological Cytoplasmic TDP-43"

Acta Neuropathologica

Authors: Adam K. Walker[1], Krista J. Spiller[1], Guanghui Ge[1], Allen Zheng[1], Yan Xu[1], Melissa Zhou[1], Kalyan Tripathy[1], Linda K. Kwong[1], John Q. Trojanowski[1,2], Virginia M.-Y. Lee[1,2,*]

Affiliations:

[1]Center for Neurodegenerative Disease Research, Department of Pathology and Laboratory Medicine, Perelman School of Medicine, University of Pennsylvania, Philadelphia, PA 19104, USA.

[2] Institute on Aging, Perelman School of Medicine, University of Pennsylvania, Philadelphia, PA 19104, USA.

*Corresponding author. E-mail: vmylee@upenn.edu. Telephone: +1-215-662-3292. Facsimile: +1-215-349-5909

Video S1 legend, and **Figs. S1-S13**

Video S1 Motor impairment and functional recovery upon hTDP-43ΔNLS suppression in rNLS mice. Video shows forelimb and hindlimb tremor in rNLS8 mouse at 6 wks off Dox, persistent hindlimb clasping behavior of rNLS8 mouse at 6 wks off Dox, and subsequent partial recovery of this phenotype in the same mouse at 2 wks back on Dox. rNLS mice are also shown with weakened limbs and difficulties walking at time points approaching disease end stage: rNLS8 mouse at 18.1 wks off Dox, rNLS9B mouse at 5.6 wks off Dox, and rNLS43 mouse at 4.3 wks off Dox

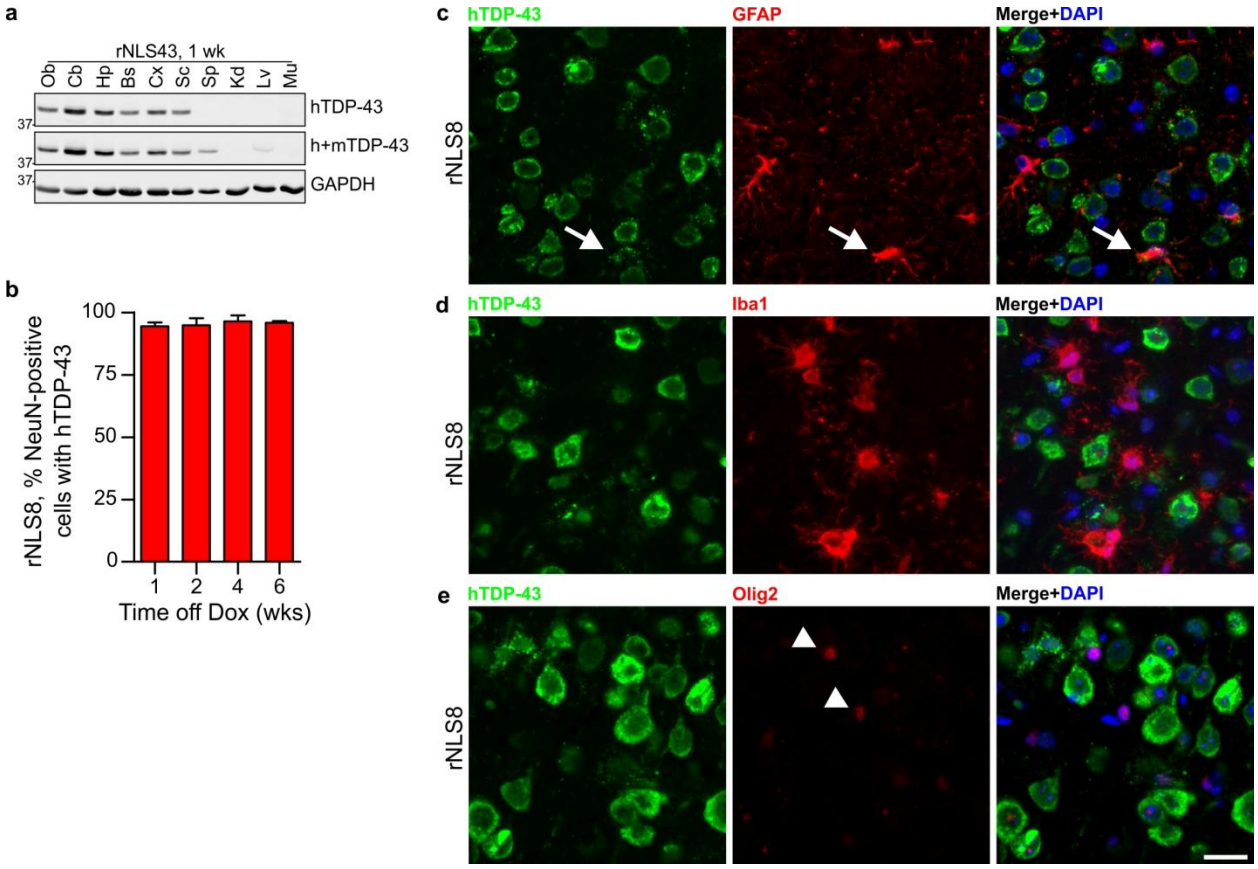

Fig. S1 Expression of hTDP-43ΔNLS in brain and spinal cord of additional line rNLS43, and analysis of neuronal and glial expression of hTDP-43ΔNLS in line rNLS8. (**a**) Expression of hTDP-43ΔNLS (hTDP-43) and total (h+m) TDP-43 protein in olfactory bulb (Ob), cerebellum (Cb), hippocampus (Hp), brainstem and remainder of the brain (Bs), cortex (Cx), spinal cord (Sc), spleen (Sp), kidney (Kd), liver (Lv) and gastrocnemius muscle (Mu) of rNLS43 mouse at 1 wk off Dox. Representative immunoblots of *n*=4. Approximate molecular weight markers in kDa are shown on the left and GAPDH is shown as a loading control. (**b**) Quantification of the percentage of NeuN-positive neurons expressing hTDP-43ΔNLS in layer V of the M1 motor cortex of rNLS8 mice at time off Dox as indicated, *n*=12 (3 mice per time point; refer to **Fig. 1h**,**i** for representative images used for quantification). (**c**) Double labeling of hTDP-43 (green) with GFAP (red) in layer V of motor cortex of rNLS8 mouse. Arrows indicate example of a $GFAP^{+}$/$hTDP\text{-}43^{+}$ cell. Double labeling of hTDP-43 (green) and (**d**) Iba1 (red) for microglia or (**e**) Olig2 for oligodendrocytes (arrowheads) in rNLS8 motor cortex. Images representative of *n*=12 (3 mice per time point of 1, 2, 4, and 6 wks off Dox). Images from 4 wks off Dox are shown. Scale bars **c**-**e** = 20μm

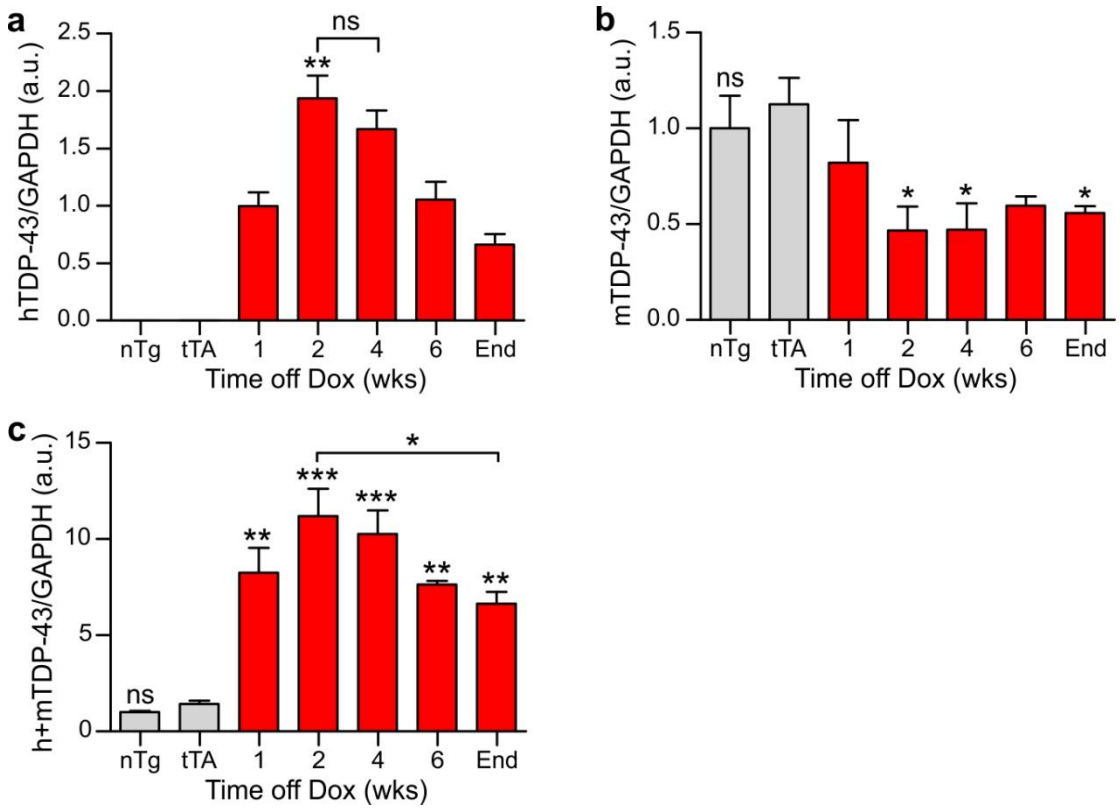

Fig. S2 Quantification of cortex h, m and h+mTDP-43 RIPA-soluble protein by IB in rNLS8 mice and controls. (**a**) hTDP-43 levels peaked at 2 wks off Dox ($p<0.01$ vs 1 wk), with no significant difference (ns) between 2 and 4 wks. (**b**) mTDP-43 levels were significantly decreased compared to monogenic control (tTA) in rNLS8 mice at 2 and 4 wks and end stage (*$p<0.05$). There was no statistically significant difference between non-transgenic control (nTg) and tTa (ns). (**c**) h+mTDP-43 levels were significantly increased compared to tTA in rNLS8 mice at all time points (**$p<0.01$, ***$p<0.001$), with a statistically significant difference between 2 wks and end stage. There was no statistically significant difference (ns) between nTg and tTa. Values are normalized to GAPDH as a loading control, and are presented as a ratio to 1 wk off Dox for hTDP-43 expression in **a**, and nTg for mTDP-43 and h+mTDP-43 in **b**,**c**, in arbitrary units (a.u.). Data analyzed by one-way ANOVA with Bonferroni's post-hoc test, *n*=3 mice for each of nTg, tTA, 1, 2, 4, and 6 wks and *n*=9 for end stage (mice at 7-18 wks). Refer to **Fig. 2a** for representative blots

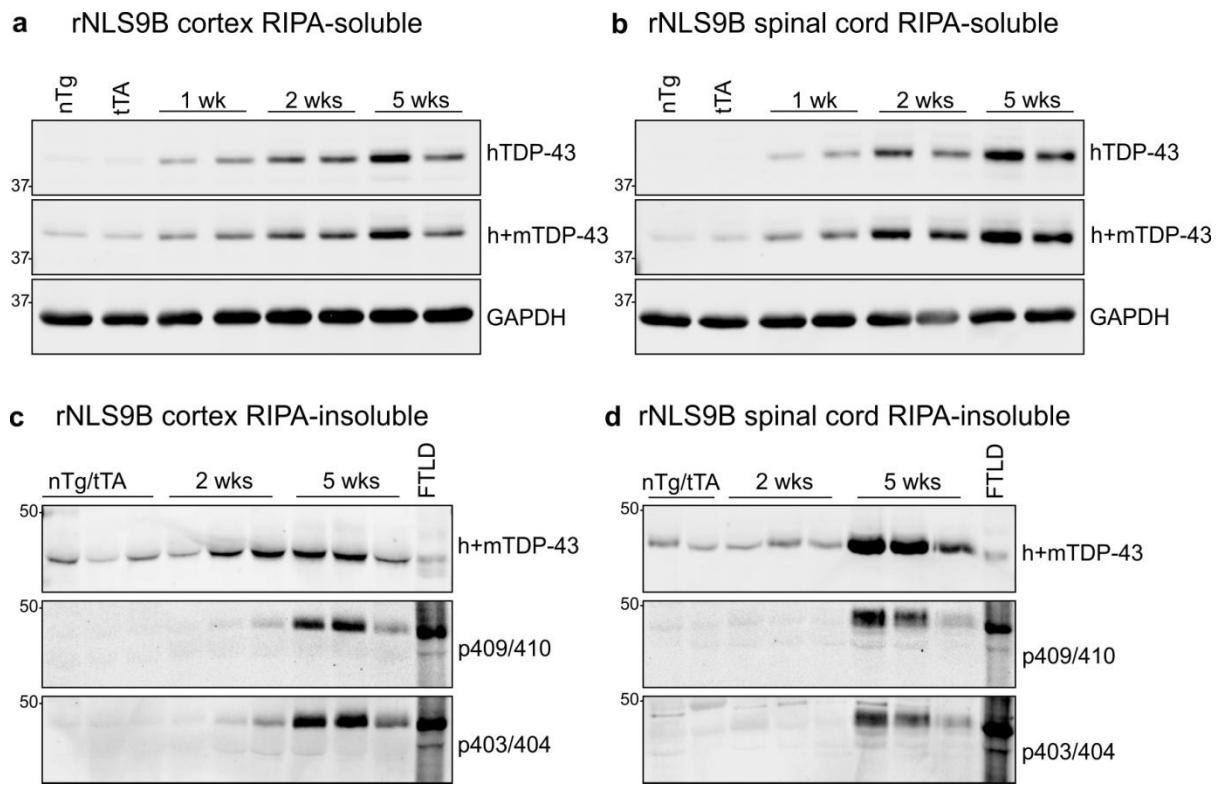

Fig. S3 rNLS9B mice express hTDP-43ΔNLS and accumulate insoluble pTDP-43 over time in the brain and spinal cord, similar to line rNLS8. (**a**,**b**) rNLS9B mice showed robust expression of RIPA-soluble hTDP-43ΔNLS with a corresponding increase in h+mTDP-43 in the cortex and spinal cord from 1 wk off Dox compared to nTg and monogenic tTA controls. (**c**,**d**) Levels of RIPA-insoluble/urea-soluble TDP-43 were variably increased at 2 wks off Dox and consistently increased at 5 wks off Dox in rNLS9B mouse cortex and spinal cord compared to nTg and tTA, with pTDP-43 variably detected in cortex at 2 wks off Dox and in all mice at 5 wks off Dox (disease end stage), and pTDP-43 detected in spinal cord only at 5 wks off Dox. Urea-soluble extract from a human FTLD patient is shown as a positive control. Each lane represents an individual mouse

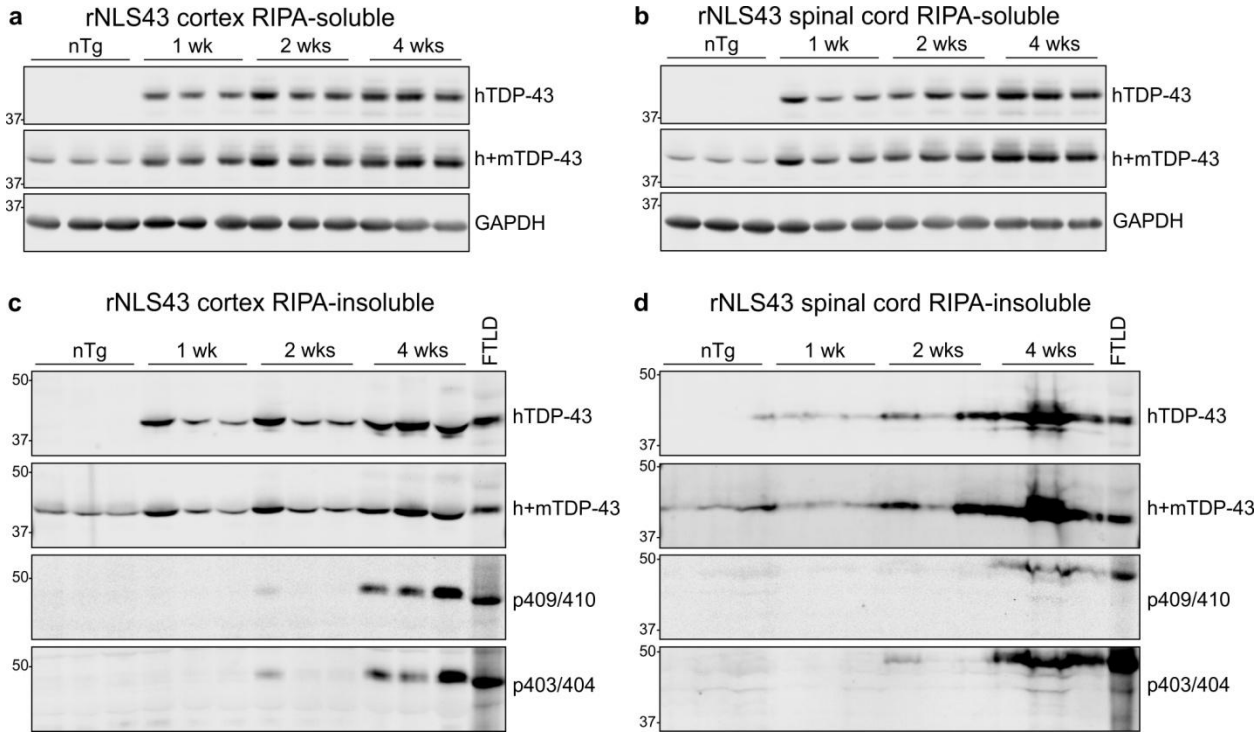

Fig. S4 rNLS43 mice express hTDP-43ΔNLS and accumulate insoluble pTDP-43 over time in the brain and spinal cord, similar to line rNLS8. (**a**,**b**) rNLS43 mice showed robust expression of RIPA-soluble hTDP-43ΔNLS with a corresponding increase in h+mTDP-43 in the cortex and spinal cord from 1 wk off Dox compared to nTg controls. Approximate molecular weight markers in kDa are shown on the left in all panels and GAPDH is shown as a loading control for RIPA-soluble samples. (**c**,**d**) Levels of RIPA-insoluble/urea-soluble TDP-43 were increased from 1 wk off Dox in rNLS43 mouse cortex and spinal cord compared to nTg controls, with pTDP-43 variably detected at 2 wks off Dox and in all mice at 4 wks off Dox (disease end stage). Urea-soluble extract from a human FTLD patient is shown as a positive control. Each lane represents an individual mouse

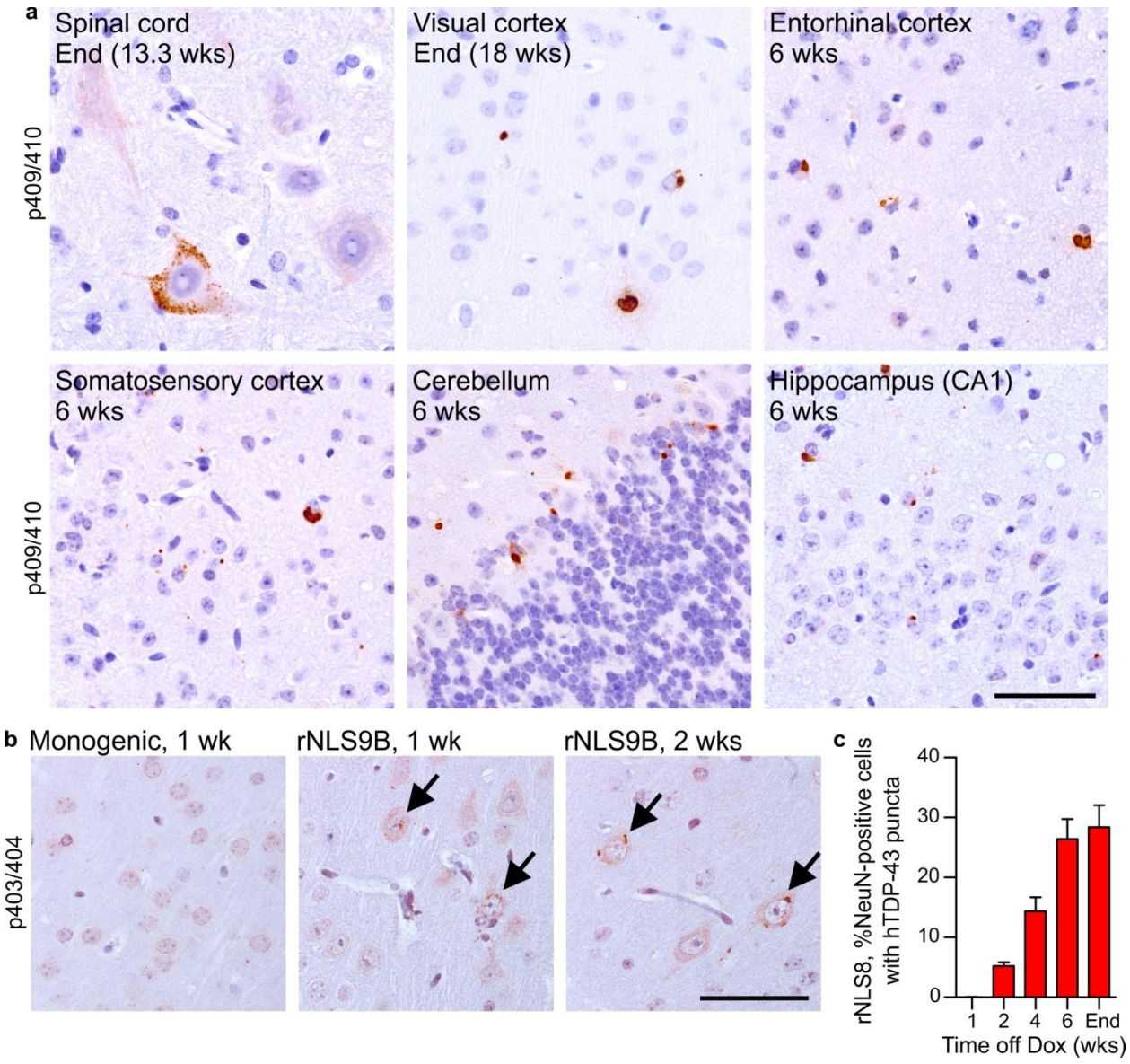

Fig.S5 pTDP-43-positive inclusions are detected in spinal cord and numerous brain regions in rNLS mice and are present as early as 1 wk off Dox, and hTDP-43-positive cytoplasmic puncta increase over time in rNLS8 motor cortex. (**a**) Inclusions and puncta positive for p409/410-TDP-43 in spinal cord, visual, entorhinal, and somatosensory cortex, cerebellum and hippocampus in rNLS8 mice. (**b**) Rare cytoplasmic puncta positive for p403/404-TDP-43 in rNLS9B layer V motor cortex at 1 wk and 2 wks off Dox (arrows). (**c**) The percentage of NeuN-positive neurons in layer V of motor cortex in rNLS8 mice with hTDP-43 positive cytoplasmic puncta over time, *n*=3 mice per time point, end stage mice at 8-18 wks (refer to **Fig. 1h**,**i** for representative images used for quantification in **c**). Scale bars **a** = 50 µm, **b** = 50 µm

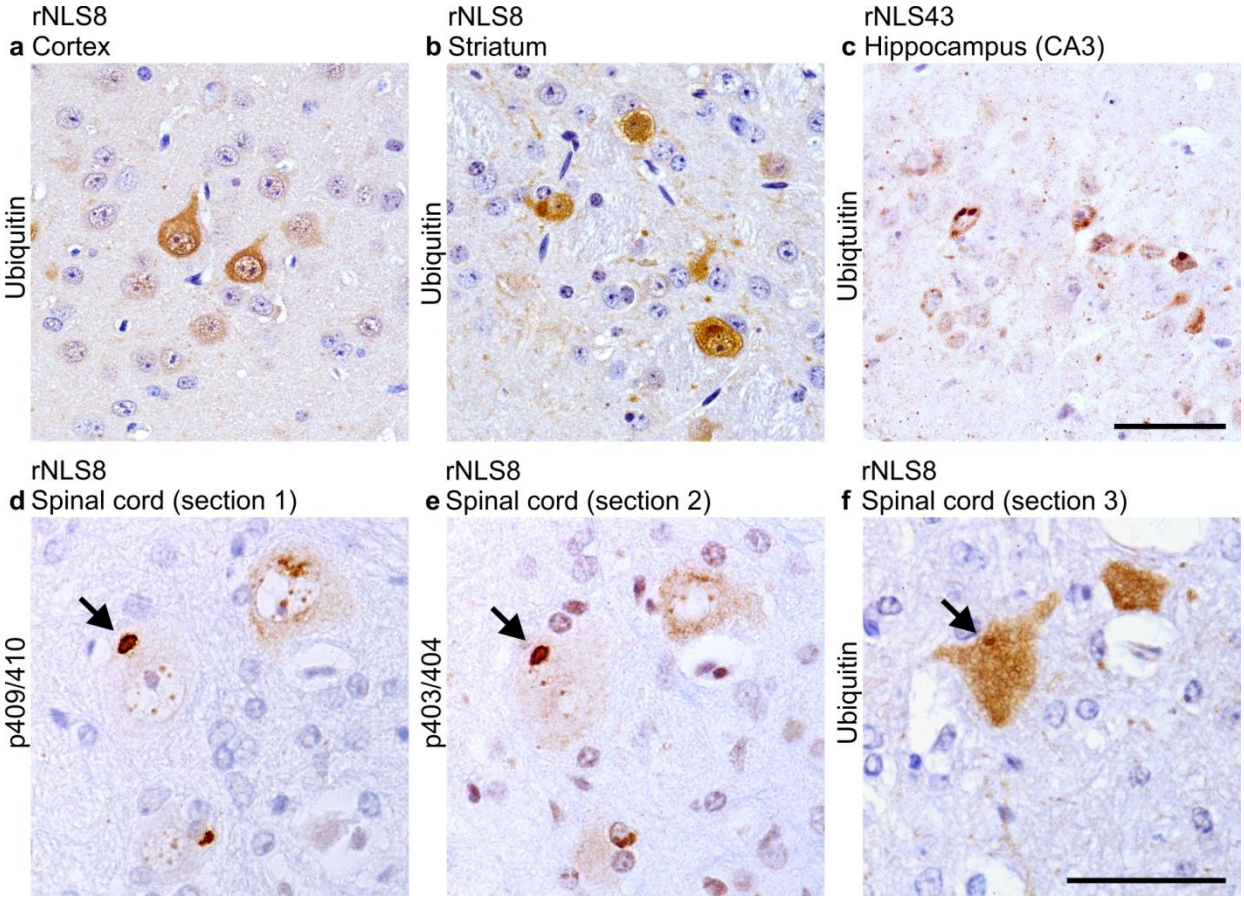

Fig.S6 Accumulation of cytoplasmic ubiquitin and ubiquitin-positive inclusions in rNLS mouse brain and spinal cord. Intense cytoplasmic ubiquitin immunoreactivity was detected in a small subset of neurons in the brain of rNLS mice, including the (**a**) cortex (layer V) and (**b**) striatum of rNLS8 mice, and (**c**) CA3 region of the hippocampus of rNLS43 mice. (**d**-**f**) In serial sections of rNLS8 mouse spinal cord, the same lumbar spinal cord motor neurons are shown to contain inclusions which co-label for p409/410 and p403/404 TDP-43 and ubiquitin (arrows), in addition to accumulation of intense cytoplasmic ubiquitin immunoreactivity. Similar ubiquitin inclusions or cytoplasmic accumulation was not seen in littermate controls (not shown). Images shown are at time off Dox of 4 wks (**a,c**), 6 wks (**b**) and end stage of 18 wks (**d**-**f**). Scale bars **a**-**c** = 50 μm, **d**-**f** = 50 μm

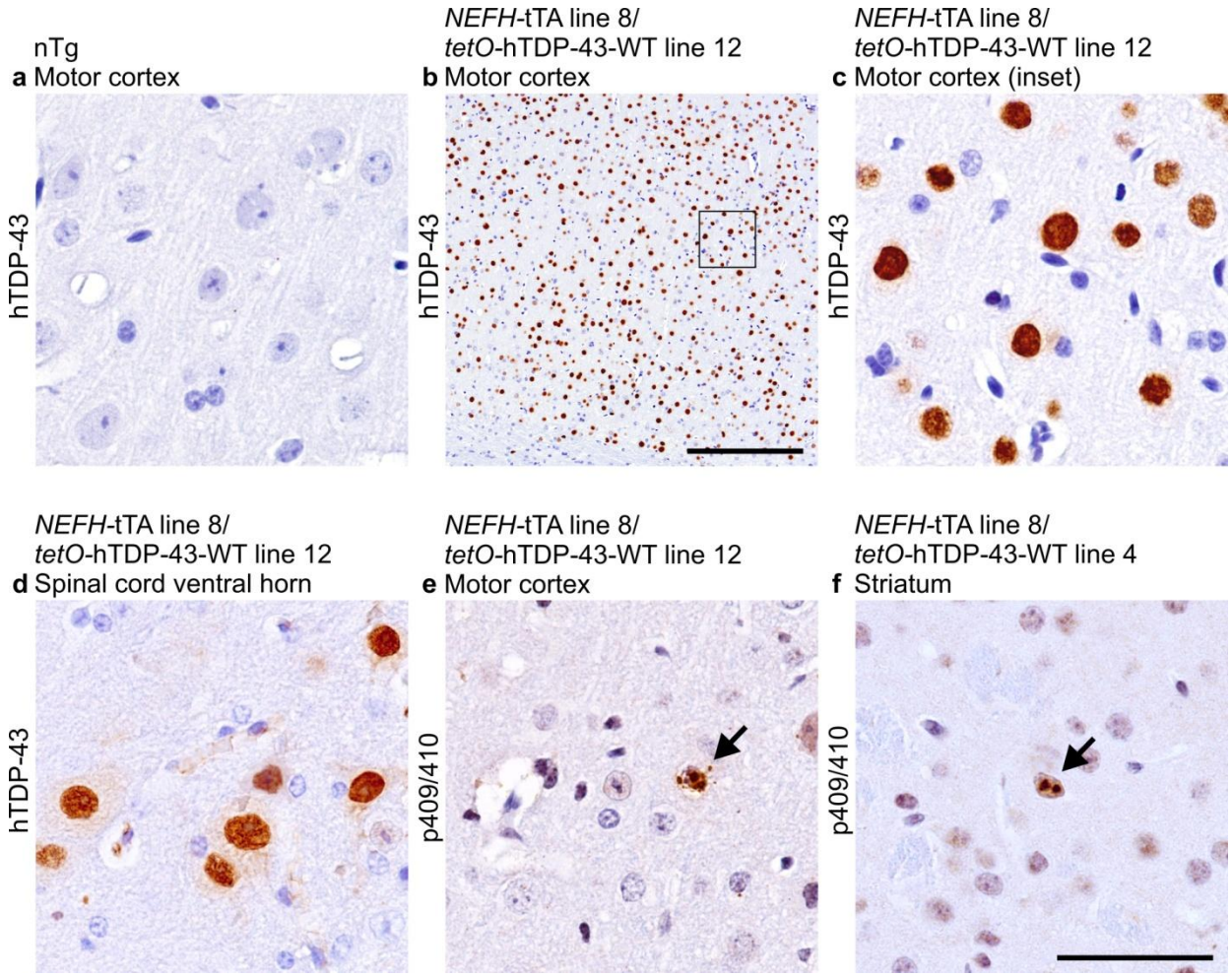

Fig. S7 Nuclear hTDP-43 is expressed broadly in the brain and spinal cord of *NEFH*-tTA/*tetO*-hTDP-43-WT mice, without formation of cytoplasmic TDP-43 pathology. (**a**) No immunoreactivity in the motor cortex of non-transgenic (nTg) littermate control mouse for hTDP-43-specific antibody, with broad detection of exclusively nuclear hTDP-43 throughout the brain, including in (**b**,**c**) motor cortex (box indicates inset shown in **c**) and also in (**d**) spinal cord of *NEFH*-tTA line 8/*tetO*-hTDP-43-WT line 12 mice. Images representative of *n*=6 bigenic mice. Similar results were obtained for bigenic *NEFH*-tTA line 8/*tetO*-hTDP-43-WT line 4 mice (*n*=7). Cytoplasmic hTDP-43 or pTDP-43-positive inclusions were not detected in any *NEFH*-tTA/*tetO*-hTDP-43-WT mice. However, extremely rare small intranuclear p409/410-positive inclusions were detected (arrows), for example in the (**e**) motor cortex of *NEFH*-tTA line 8/*tetO*-hTDP-43-WT line 12 mice and (**f**) striatum of *NEFH*-tTA line 8/*tetO*-hTDP-43-WT line 4 mice. Images shown are at time off Dox of 6 wks (**a-c**,**e**), 6 months (**d**) and 4 wks (**f**). Scale bars **a**, **c**-**f** = 50 μm, **b** = 250 μm

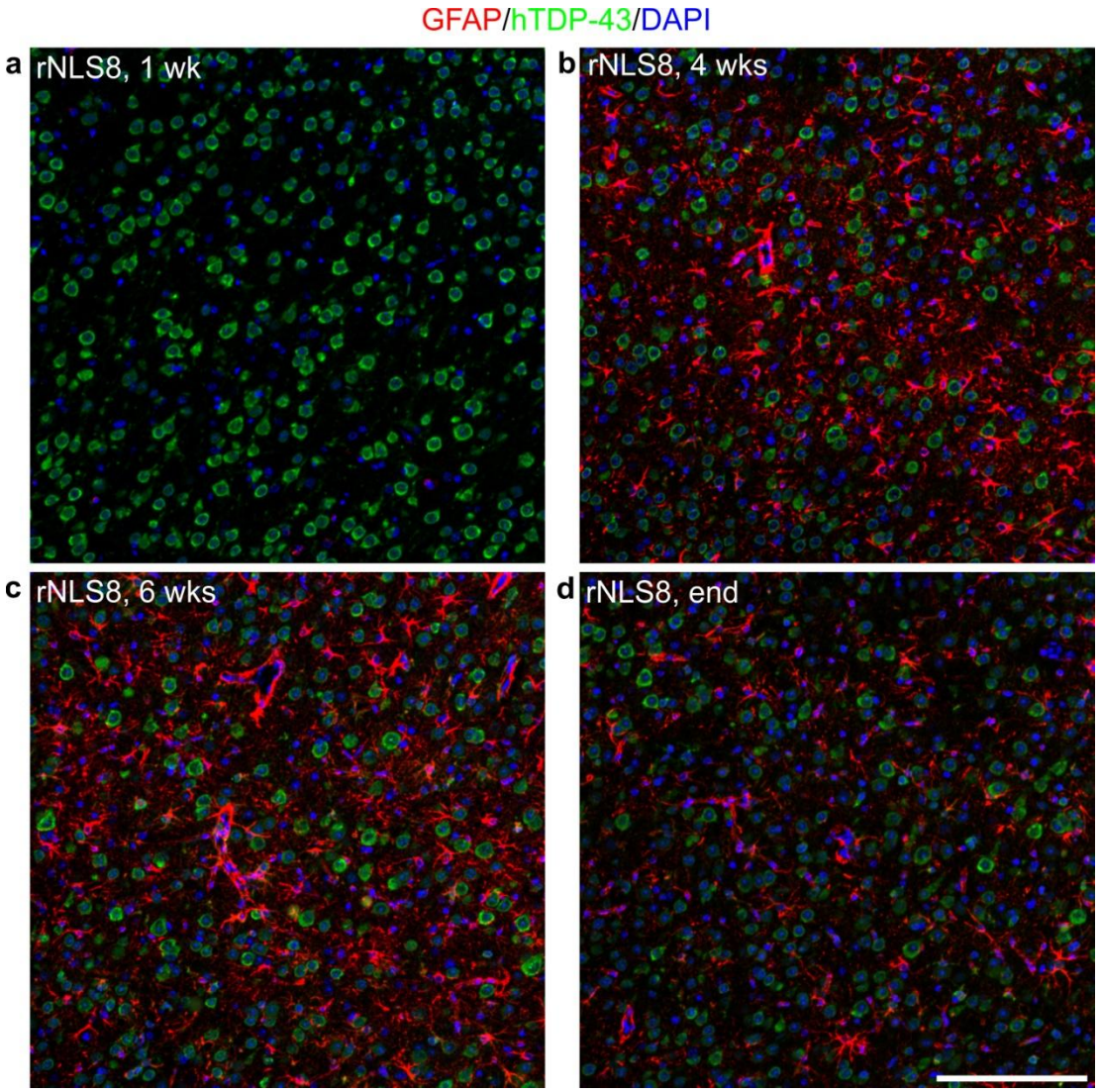

Fig. S8 Astrogliosis develops in a time-dependent manner in rNLS8 mouse motor cortex. (**a**) Double labeling for GFAP showed no evidence of astrogliosis by immunofluorescence (red) in rNLS8 mouse motor cortex at 1 wk off Dox, despite widespread expression of hTDP-43ΔNLS (green). (**b**-**d**) However, marked astrogliosis became evident at 4 wks off Dox and was maintained at 6 wks off Dox and then diminished towards disease end stage (image for 18 wks shown). Images are representative of *n*=3 at each time point. Scale bar **a**-**d** = 100μm

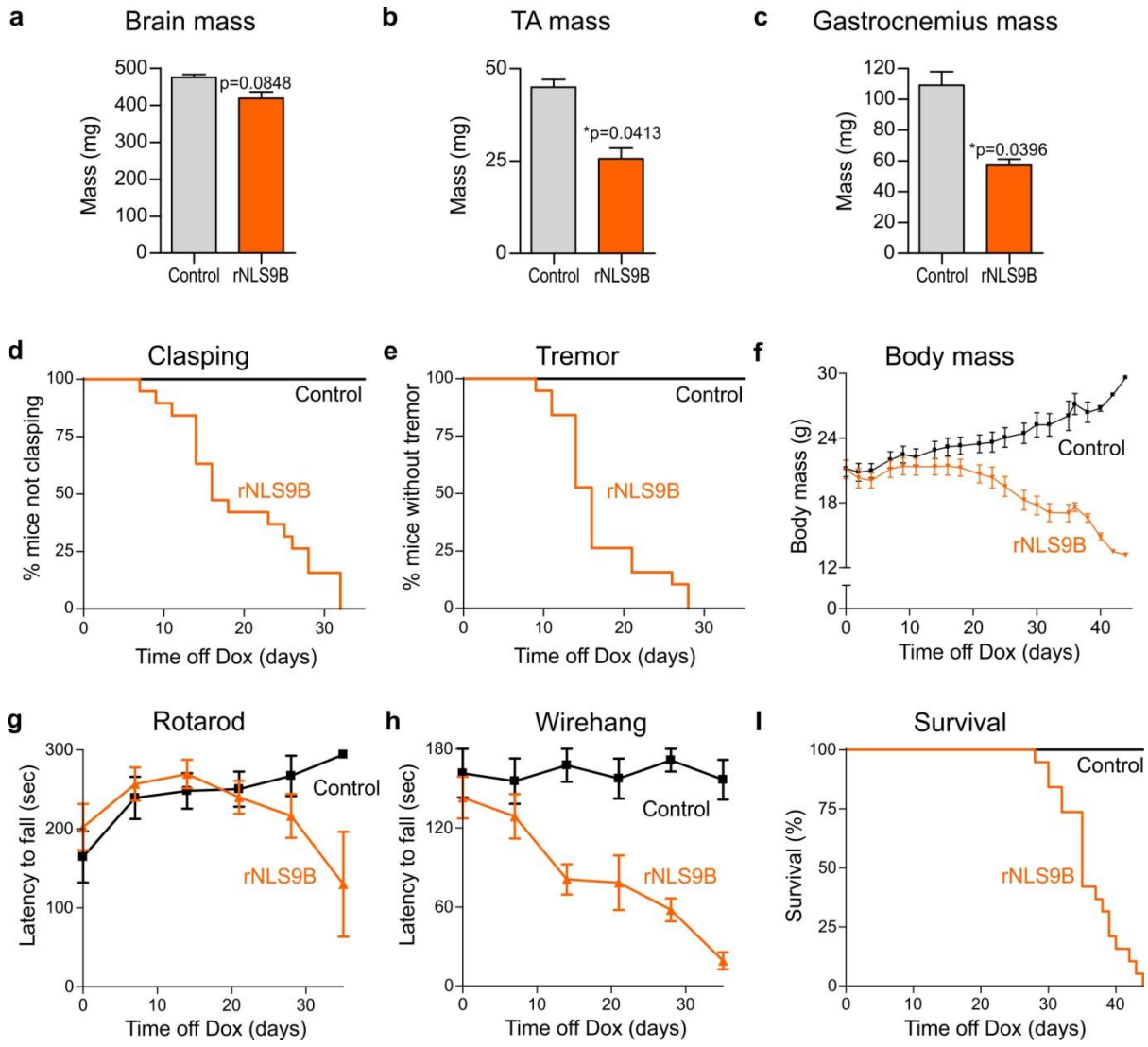

Fig. S9 Analyses of brain, muscle and body masses, motor phenotype, and survival in rNLS9B mice. Mass of fresh dissected (**a**) brain, (**b**) TA muscle, and (**c**) gastrocnemius muscle of female rNLS9B mice at disease end stage (~5 wks off Dox) and nTg or tTA monogenic littermate controls, *n*=3 per group, significance determined by paired two-tailed t-test. (**d**,**e**) Onset of hindlimb clasping and fine forelimb and/or hindlimb tremor in rNLS9B mice. (**f**) Change in body mass over time in rNLS9B mice. (**g**) Decline in motor performance on rotarod test and (**h**) progressive decline in grip strength as measured by wirehang test in rNLS9B mice. (**i**) Decreased survival in rNLS9B mice. For **d**-**f** and **i** *n*=14 controls, *n*=19 bigenic, and for **g**,**h** *n*=9 controls, *n*=11 bigenic. Both males and females are included in **d**-**i**

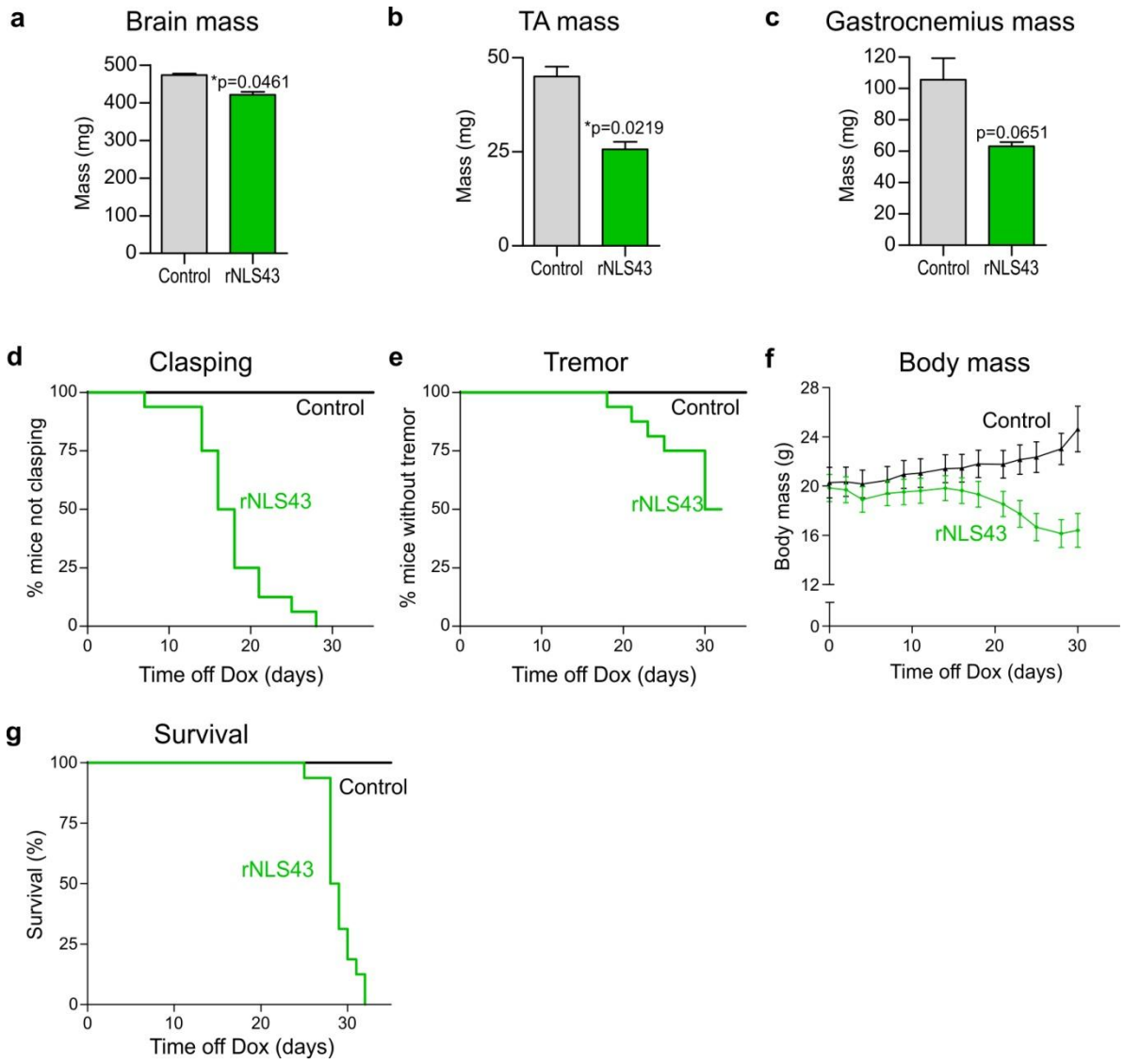

Fig. S10 Analyses of brain, muscle and body masses, motor phenotype, and survival in rNLS43 mice. Mass of fresh dissected (**a**) brain, (**b**) TA muscle, and (**c**) gastrocnemius muscle of female rNLS43 mice at disease endstage (~4 wks off Dox) and nTg or monogenic littermate controls, *n*=3 per group, significance determined by paired two-tailed t-test. (**d**,**e**) Onset of hindlimb clasping and fine forelimb and/or hindlimb tremor in rNLS43 mice (only 50% of rNLS43 mice developed tremor prior to disease end stage). (**f**) Change in body mass over time in rNLS43 mice. (**g**) Decreased survival in rNLS43 mice. For **d**-**g**, both males and females are included and *n*=14 controls, *n*=16 bigenic

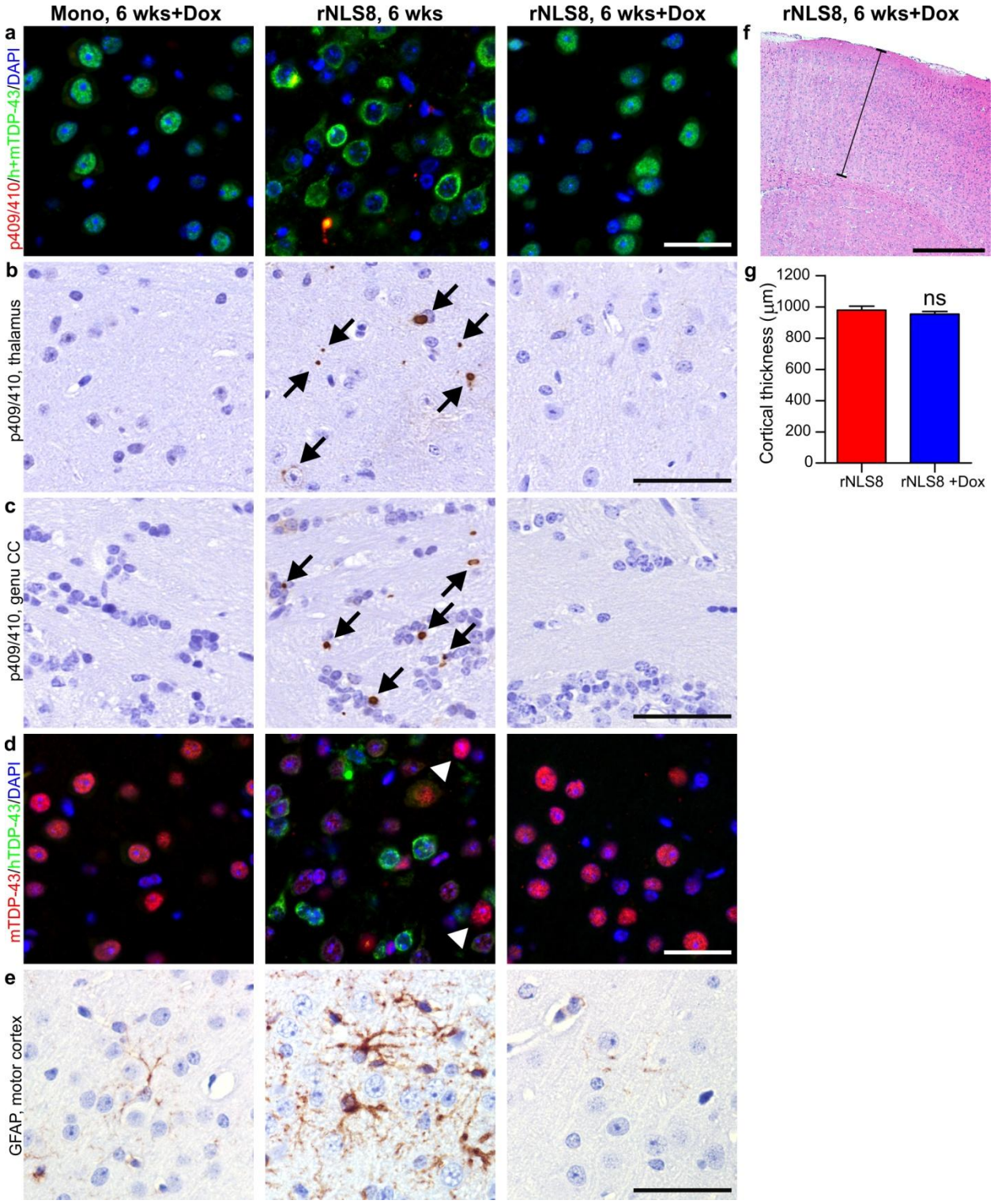

Fig. S11 Clearance of pTDP-43 pathology, return of nuclear TDP-43 and resolution of astrogliosis in rNLS8 mice after reintroduction of Dox to suppress hTDP-43ΔNLS expression, without recovery in cortical thickness. (**a**) p409/410-TDP-43 (red) and cytoplasmic h+mTDP-43 (green) were detected in layer V motor cortex of rNLS8 mouse at 6 wks off Dox but not in monogenic hTDP-43ΔNLS (Mono) control and

rNLS8 mouse at 18 wks +Dox. Note the return of nuclear h+mTDP-43 immunoreactivity in rNLS8 +Dox. Similarly, p409/410-TDP-43 was not detected in the brain, including the (**b**) thalamus and (**c**) genu of the corpus callosum (CC), following Dox reintroduction. (**d**) Nuclear mTDP-43 (red) levels decreased in cells expressing hTDP-43 (green) in motor cortex of rNLS8 mouse off Dox at 6 wks, but were maintained in cells not expressing hTDP-43 (arrowheads), and mTDP-43 returned to control levels in mice at 18 wks +Dox. (**e**) Marked astrogliosis was detected in layer V of the motor cortex in rNLS8 mice at 6 wks off Dox, but not in littermate rNLS8 at 18 wks +Dox. Results are representative of $n \geq 3$ mice per group with mice analyzed at 12-32 wks +Dox. (**f**) Measurement of cortical thickness in the motor cortex at Bregma 1.10. Shown is H&E image of rNLS8 mouse at 32 wks +Dox. (**g**) Quantification of cortical thickness of rNLS8 mice at 6 wks off Dox ('rNLS8', $n=3$) compared to rNLS8 mice at 12-32 wks +Dox ('rNLS8 +Dox', $n=5$). There is no statistically significant difference (ns) by two-tailed t-test. See also **Fig. 3a**-**c**. Scale bars **a**-**e** = 50 μm, **f** = 500 μm

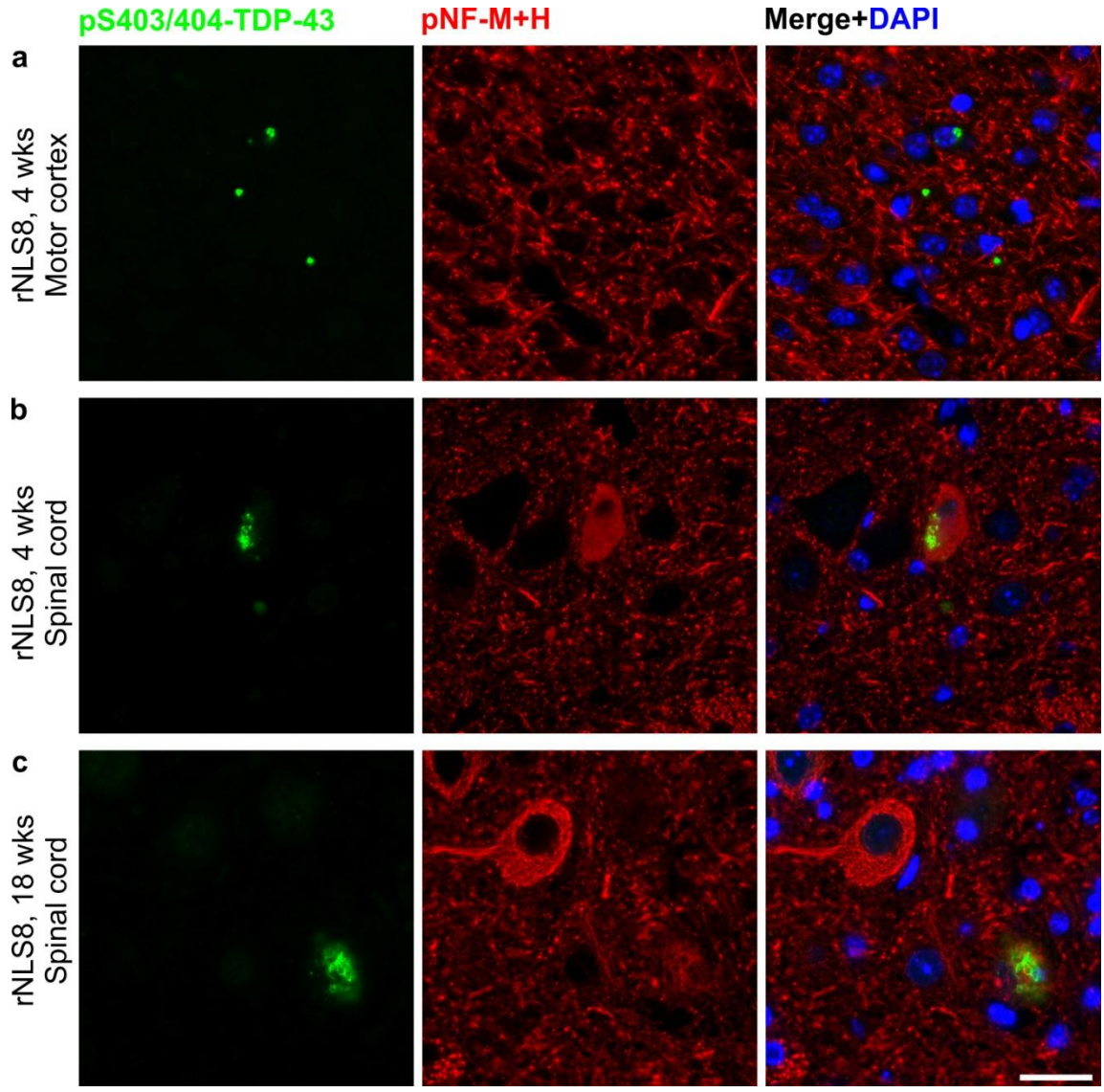

Fig. S12 Phospho-TDP-43 pathology in brain and spinal cord of rNLS8 mice does not co-localize with neurofilament proteins. Double labeling IF for phospho-S403/404-TDP-43 and phosphorylated neurofilament medium and heavy chains (pNF-M+H, antibody TA51) shows little or no accumulation of neurofilament proteins in TDP-43 pathology in (**a**) motor cortex of rNLS8 at 4 wks off Dox, (**b**) spinal cord of rNLS8 at 4 wks off Dox, and in (**c**) spinal cord of rNLS8 at end stage (18 wks off Dox shown). Scale bar **a**-**c** 25µm

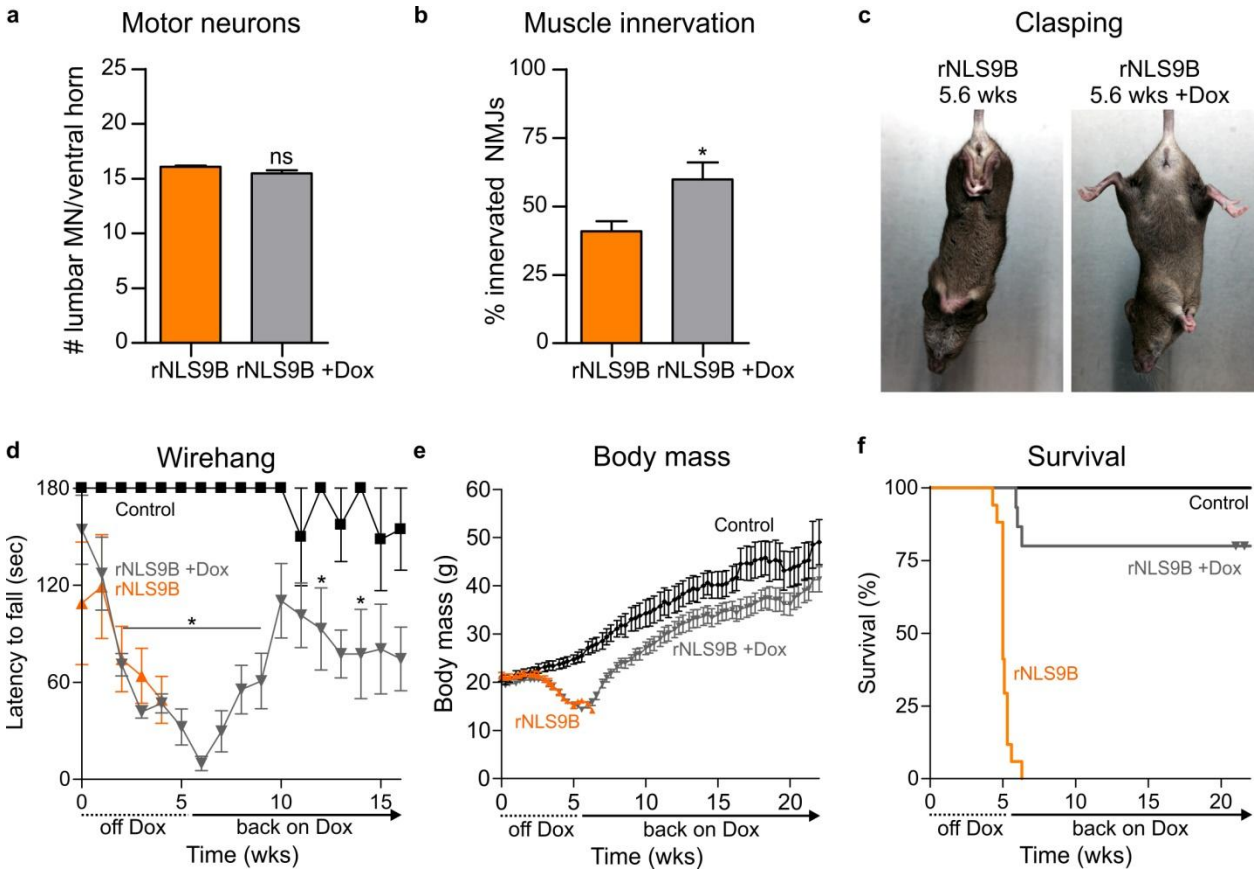

Fig. S13 Suppression of hTDP-43ΔNLS expression rescues motor phenotypes and restores lifespan in rNLS9B mice. (**a**) rNLS9B mice returned to Dox at 5.6 wks for 4 months showed no significant difference in motor neuron number compared to rNLS9B mice killed at 5.6 wks, and (**b**) had significantly more innervated NMJs, *p<0.05, *n*=4 rNLS9B mice at 5.6 wks, *n*=3 rNLS9B mice at 5.6 wks +4 months back on Dox. (**c**) All rNLS9B mice displayed persistent hindlimb clasping (left image). However, as early as 2 wks after the reintroduction of Dox at 5.0-6.0 wks, 12 of 15 rNLS9B mice showed partial recovery of this phenotype (right image, showing the same mouse at 4 wks back on Dox). (**d**) Reintroduction of Dox at 5.6 wks also resulted in a functional recovery in the wirehang test, *p<0.05 versus nTg/monogenic littermate controls by two-way ANOVA with Bonferroni's post-hoc test, *n*=3 controls (black line), *n*=5 rNLS9B mice +Dox at 5.6 wks (gray line), *n*=3 rNLS9B littermate mice not returned to Dox (orange line). (**e**) Reintroduction of Dox at 5.0-6.0 wks (*n*=15) also dramatically reversed the weight loss which reached a nadir at 6 wks in rNLS9B mice, compared to mice maintained off Dox (*n*=17, some also shown in **Fig. S9l**). (**f**) Without Dox, all 17 rNLS9B mice reached disease end stage between 4.3 and 6.3 wks, with a median survival of 5.0 wks. When Dox was reintroduced three mice reached end stage (at 5.9-6.3 wks from initial Dox removal), and 12 mice survived ≥4 months longer. The survival curves of rNLS9B mice off Dox and back on Dox are significantly different at ***p<0.001 by log rank test. Triangles indicate censored animals either killed for analysis or remaining alive